01,07,08

Structure evolution during the transformation of Si into SiC by the method of coordinated substitution of atoms

© S.A. Kukushkin[1], M.G. Vorobev[1], A.V. Osipov[1], A.S. Grashchenko[1], E.V. Ubyivovk[1,2]

[1] Institute for Problems in Mechanical Engineering of the Russian Academy of Sciences, St. Petersburg, Russia
[2] St. Petersburg State University, St. Petersburg, Russia

E-mail: sergey.a.kukushkin@gmail.com

Received May 14, 2024
Revised May 14, 2024
Accepted May 15, 2024

Using the example of the formation of epitaxial silicon carbide (SiC) layers on silicon (Si) by the method of coordinated substitution of atoms, studies have been conducted on the evolution of the structure during phase transformations in multicomponent crystals with chemical reactions. A significant change over time in the microstructure and properties of the formed SiC layers was observed. The microstructure and properties of the SiC/Si layers were analyzed using the method of photoluminescence (PL), reflection high-energy electron diffraction (RHEED), the method of spectroscopic ellipsometry (SE), and the evolution of the structure of the SiC-Si interface boundary was studied using the method of scanning electron microscopy (SEM). It was found that during the first five minutes of synthesis, a change in the reconstruction of the SiC surface occurs, moreover, elastic deformations change from compressive to tensile. It was also found that during the synthesis of SiC on Si(111), both a (3×3) and a (2×1) reconstruction can form on the SiC surface.

Keywords: silicon carbide on silicon, surface reconstruction, topochemical reactions, elastic deformation, photoluminescence, diffusion zone, nanostructures, microstructure evolution, AlN, GaN, AlGaN.

DOI: 10.61011/PSS.2024.07.58982.120

1. Introduction

In a set of studies, summarized in papers [1–5], a brand new method of synthesis of thin epitaxial SiC films on Si substrates was developed differing from the standard films growth methods. With the growth of silicon carbide on silicon complying with standard methods [6–10] the precursors containing carbon and silicon atoms, from which SiC film arises, come from the outer environment onto the substrate surface. In method, offered in [1–5], the growth of SiC films on Si occurs due to substitution of half of silicon atoms with carbon atoms in the surface layer of the silicon substrate. Specific feature of the substitution process is that replacement of Si atoms by C atoms occurs in the coordinated way, i. e. new chemical bonds are formed simultaneously and in line with destruction of old bonds, which results in preservation of the common diamond-like structure of chemical bonds (Figure 1). The reason of this coordination is that the energy of activated state Si-O-C is about 2 times less than the bond breakage energy Si-Si.

To carry out the coordinated substitution of atoms a chemical reaction between the gaseous carbon monoxide (CO) and the silicon substrate surface is used

$$2\mathrm{Si}(cr) + \mathrm{CO}(gas) = \mathrm{SiC}(cr) + \mathrm{SiO}(gas) \uparrow . \quad (1)$$

This coordinated substitution of atoms is possible only in case of reaction (1). The reason is that the reaction (1) proceeds in two stages. At the first stage of reaction the CO molecule interacts with the silicon substrate surface and is adsorbed on it [11]. After that, the bonds C-Si and C-O start to get a steep inclination, oxygen atom enters into chemical reaction with Si atom resulting in the formation of C-O-Si triangular structure which corresponds to the transition state or activated state [11]. At the second stage C atom is entrapped inside the silicon structure, and Si atom linked with O and C, on the contrary, is expelled from Si, and an adsorbed molecule of SiO is formed, which is removed from the system, and an excited carbon C released from CO molecule after chemical reaction is displaced towards the temporary location in the silicon lattice. The intermediate state „pre-carbide silicon“ is formed at this stage [1–5,11].

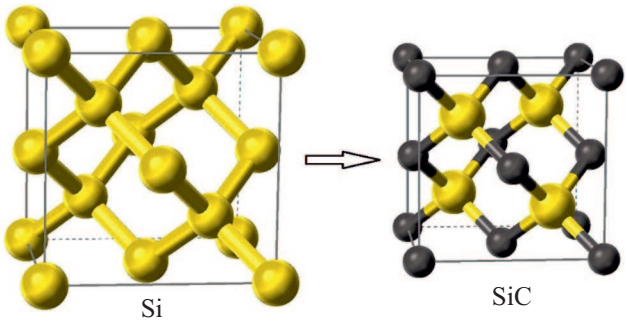

Figure 1. Transformation of silicon structure into silicon carbide with conservation of chemical bonds.

Carbon atoms at this stage form a meta-stable ordered structure near the silicon surface with a barrier height of several kT. At the final reaction stage „pre-carbide silicon" is packed into a more dense structure of silicon carbide. Such transformation is always accompanied by the formation of voids, since the volume of the Si cell is two times larger than the volume of the SiC cell. Theoretical approaches to description of this process and appropriate experimental data are provided in details in papers [1–5] and in original studies the references to which are given in these reviews. To improve the quality of crystals of SiC films silane (SiH_4) is added to CO gas [3]. Silane is a source of additional silicon compensating the silicon vacancies formed earlier. Due to adding SiH_4 into the system the probability of silicon vacancies formation in the near-surface silicone layers is reduced, and, thus, the driver of shrinkage pores formation is reduced.

It should be noted that the displacement proceeds in layers, i. e. several layers of pre-carbide silicon are simultaneously transformed into SiC with the film shifting perpendicular to the substrate surface. As a result, the SiC film is formed sufficiently uniform in thickness and without noticeable voids. All voids end up in silicon under the film SiC [1–5]. It is interesting to note that the distance between the atoms C lying along the plane (111), projected onto the plane $(11\bar{2})$, in SiC is 3.08 Å. Thus, the distance between the planes of five cells in SiC $\sim$ 15.4 Å up to the first decimal place coincides with the distance between the planes of four cells Si $\sim$ 15.4 Å. This means that when an intermediate state is converted into silicon carbide, not all bonds are broken, but only those that do not match the bonds in Si [1,12]. At the same time, an empty space is formed under the place where the bonds were broken. It is for this reason that on the final stage the elastic deformations in the SiC [1,12] layer are almost completely absent. However, since the process of Si transformation into SiC takes place over some period of time, deformations may occur at different stages of transformation and the morphology of the SiC surface may change. In addition, since the upper layer of the Si substrate plane undergoes shrinkage when converted to SiC, shrinkage pores may form on the surface [1]. The latter affect the distribution of elastic deformations in the SiC film during growth. Also, the morphology and stresses in SiC are influenced by temperature, reactor pressure, conductivity and orientation of the Si substrate [3].

The studies of evolution of SiC microstructure and Si domain directly contacting the SiC-Si phase interface are a complex problem of high fundamental value because all stages of phase transformation of one solid substance into another under the action of chemical reactions now can be traced. The study of these processes is also of applied relevance. Thus, the latest research [13–16] has demonstrated that SiC/Si hybrid structures may be successfully used as a substrate material to grow various kinds of AlN, GaN, AlGaN heterostructures and may serve as the basis for the fabrication of light-emitting diodes and transistors with high mobility of the charge carriers, and spintronics devices [13,16]. For these purposes we need SiC/Si substrates with a clearly defined structure of SiC surface layer, with a defined SiC/Si inter-phase boundary, appropriate thickness of SiC layer and minimal possible roughness.

In studies [14,15] the microstructure evolution of SiC layers on Si have been initiated. Thus, in study [14] the evolution of SiC/Si microstructure in pure CO environment was analyzed, and in study [15] — in CO and SiH_4 gas mixture environment. These studies demonstrated that irrespective of whether the synthesis process takes place in pure CO or in a mixture of CO and SiH_4, on a certain stage of SiC growth the compressive elastic stresses occur that after some time are replaced with the tensile stresses. The difference arises only in the moment of time when the stresses sign is changed. In studies [14,15] the microstructure evolution was analyzed by method of X-ray diffractometry (XRD), method of total external reflection of X-rays (TER) and method of Raman scattering (RS). However, these studies didn't allow to fully clarify the mechanisms occurring in SiC film formation. In particular, we still don't know what happens at different moments of synthesis with SiC microstructure and Si at the interface SiC-Si. Also it is unclear if SiC/Si surface reconstruction occurs. In this study it is suggested to trace both, the evolution of microstructure of SiC film itself, and evolution of microstructure of Si domain directly adjacent to SiC-Si phase interface. The analysis of microstructure will be carried out using photoluminescence method (PL), Reflection high-energy electron diffraction (RHEED), spectroscopic ellipsometry (SE) method. The evolution of SiC-Si phase interface will be studied by method of scanning electron microscopy (SEM).

2. Synthesis methods

SiC films were grown on the surface of faces (111) of Si plates of *p*-type and *n*-type of conductance in the following time periods: 1, 3, 5, 20 and 40 min, similar to the way it was done in paper [16]. Before growing of SiC the surface of Si plates was cleaned from possible organic impurities, foreign micro-particles, metal ions and anions. A layer of silicon oxide was removed from the surface of Si plates, after that the surface was passivated with hydrogen. The process of Si surface cleaning and passivation was carried out according to method [17]. SiC was growing at a temperature of 1270°C in the gas mixture of CO and SiH_4 with flow intensities $Q_{CO} = 12$ ml/min and $Q_{SiH_4} = 3$ ml/min. Cumulative pressure of gas mixture of CO and SiH_4 during the growth process was $p_{CO+SiH_4} = 360$ Pa. The process of synthesis in each of the time intervals (1, 3, 5, 20 and 40 minutes) was carried out simultaneously on substrates of *p*-type, and *n*-type of conductance, i. e. the substrates were located in the reactor in similar growth conditions.

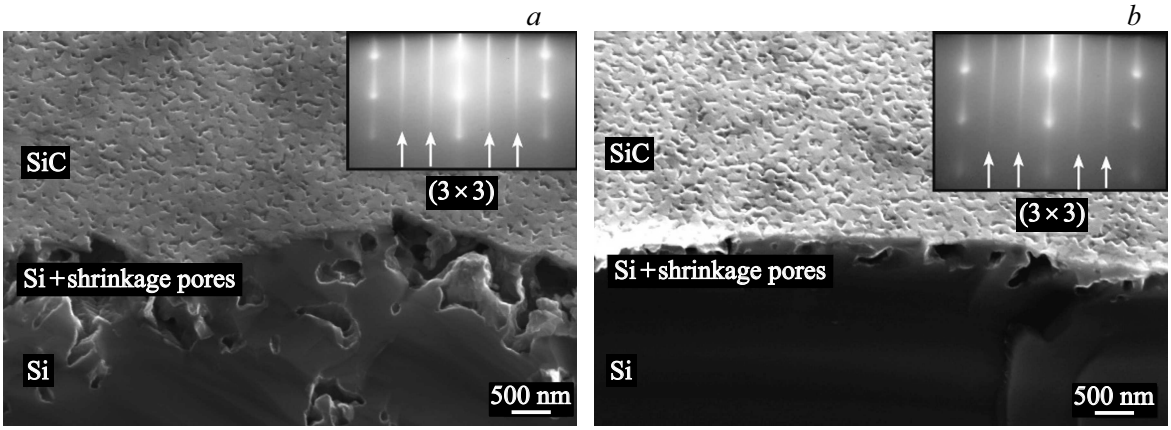

Figure 2. Images of the cross-sectional fractures of samples SiC/Si(111), synthesized for 1 min made using SEM; *a* — Si substrate of *p*-type of conductance; *b* — Si substrate of Si−*n*-type of conductance; the insert windows in the Figure illustrate the electron diffraction patterns taken from the samples surface in azimuth ⟨110⟩ and reconstruction type (3 × 3); the arrows show third order diffraction streaks.

The microstructure was analyzed using the four methods decsribed below: PL, RHEED, SEM and SE. The photoluminescence spectra were measured using Accent RPM Sigma device at a temperature of 77 K. Procedure of experimental data post-processing included smoothing of noise and searching of maximums with the help of analytical software Fityk. Nd:YaG laser with an output power of 0.9 mW was used as a luminescence excitation source. The diffraction patterns of the high-energy electrons were obtained using EMR-100 electron diffraction apparatus with the electrons energy of 50 keV. Images of the end-face cuts were obtained using scanning-electron microscope JEOL JSM 7001F. The ellipsometric spectra were obtained using WVASE^{TM} (0.7−6.4 eV) ellipsometer by J.A. Woollam Inc.

3. Experimental findings and their analysis

3.1. Microscopy of SiC-Si phase interface

Figures 2−5 illustrates the SEM images of the cross-sectional fractures of SiC/Si samples synthesized in different time. The inserts in these figures show the electron diffraction patterns corresponding to these images obtained by means of RHEED from the surface of these samples.

3.2. Dependences of density and average size of pores in Si in the domain adjacent to the phase interface SiC-Si

Figure 6, *a* and *b* show the graphs of dependencies of density and average size of pores in SiC/Si(111) samples' cross-sectional fractures. The average size of pores was analyzed from the micro-photos of the samples' cross-sectional fractures (Figures 2−5) on an area of 1 μm^2.

3.3. Dependence of average thicknesses of SiC films in SiC/Si(111) samples and average width of the diffusion zone boundary on synthesis time

Figure 7, *a, b* illustrates the dependencies of average thicknesses of SiC films in SiC/Si(111) samples and dependencies of diffusion zone boundary from the synthesis time as obtained from the microscopic images of the same series as images shown in Figures 7−10. The diffusion zone boundary means the interface of porous and non-porous zones in Si substrate. This boundary can be seen from the micro-photos in Figures 2−5.

Ellipsometric spectra of SiC/Si(111) samples grown on Si with *n*-type and *p*-type of conductance are not shown here because of small space in the page. We should only note that behavior of average density of pores and average thickness of SiC films based on ellipsometric data of SiC/Si(111) samples synthesized on Si of *p*- and *n*-types of conductance is practically the same and only slightly differs from the dependencies given in Figures 6, 7.

3.4. Photoluminescence spectra

Figure 8 shows the smoothed PL spectra of SiC/Si samples synthesized at different time. In these spectra we may observe the peaks within the ranges 395−405 and 470−500 nm of various intensity and width. Apart from it, on the substrates grown for 3 and 40 min, the peaks in 600−630 nm area are observed. Figure 8, *a* show the PL spectra of SiC samples on Si(111) substrates of *p*-type; Figure 9, *b* shows the PL spectra of SiC samples on substrates Si(111) of *n*-type. Because for samples synthesized for 3 min, especially for the sample grown on Si of *n*-type of conductance we may observe the sufficiently sharp peaks in 623.05 and 630.26 nm area, the PL spectrum of SiC sample synthesized on Si substrate of *n*-type of

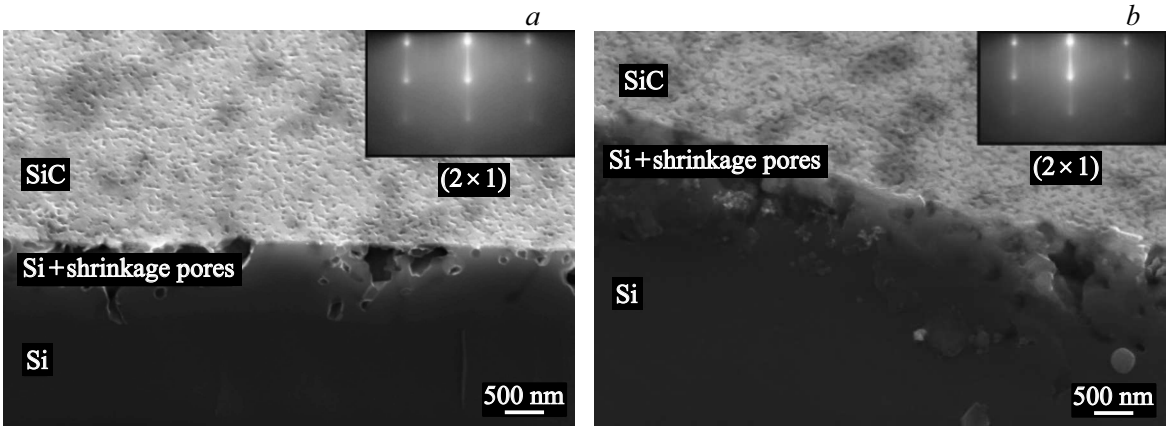

Figure 3. Images of the cross-sectional fractures of samples SiC/Si(111), synthesized for 3 min made using SEM; *a* — Si substrate of *p*-type of conductance; *b* — Si substrate of Si−*n*-type of conductance; the insert windows in the Figure illustrate the electron diffraction patterns taken from the samples surface in azimuth ⟨110⟩ and reconstruction type (2×1).

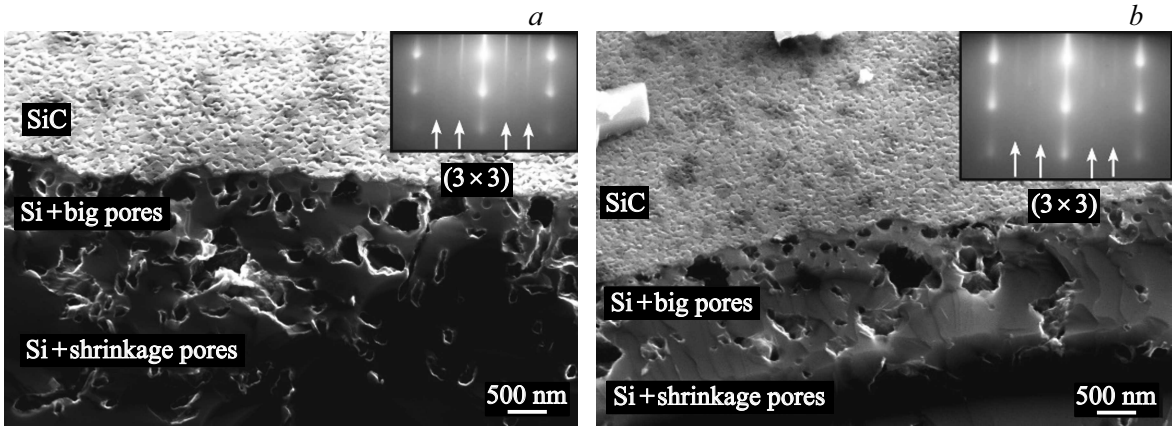

Figure 4. Images of the cross-sectional fractures of samples SiC/Si(111), synthesized for 5 min made using SEM; *a* — Si substrate of *p*-type of conductance; *b* — Si substrate of Si−*n*-type of conductance; the insert windows in the Figure illustrate the electron diffraction patterns taken from the samples surface in azimuth ⟨110⟩ and reconstruction type (3×3); the arrows show third order diffraction streaks.

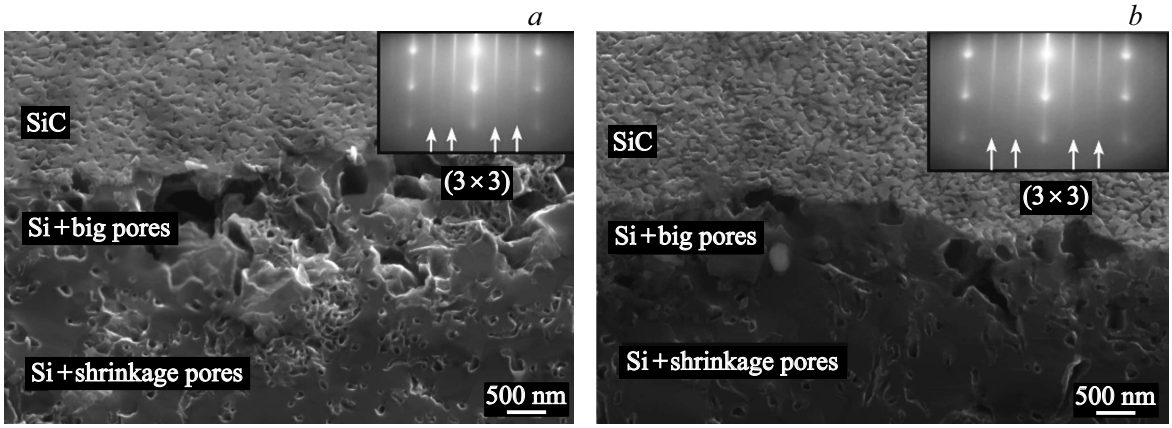

Figure 5. Images of the cross-sectional fractures of samples SiC/Si(111), synthesized for 40 min made using SEM; *a* — Si substrate of *p*-type of conductance; *b* — Si substrate of Si−*n*-type of conductance; the insert windows in the Figure illustrate the electron diffraction patterns taken from the samples surface in azimuth ⟨110⟩ and reconstruction type (3×3); the arrows show third order diffraction streaks.

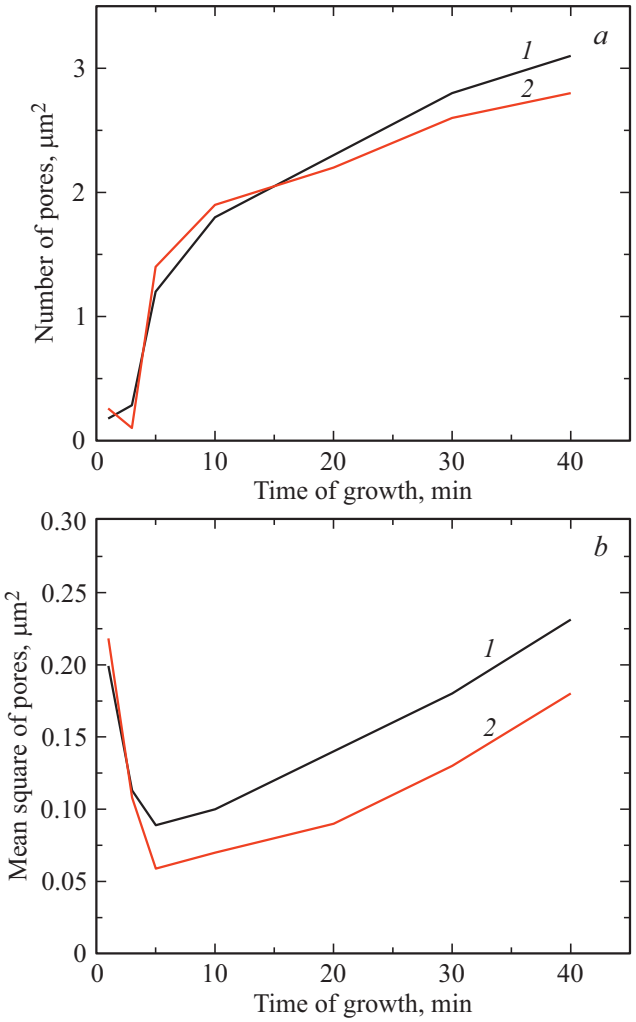

Figure 6. *a* —average density of pores in SiC/Si(111) samples versus synthesis time; *1* — SiC/*p*-Si samples; *2* — SiC/*n*-Si samples. *b* — average area of voids in SiC/Si(111) samples versus synthesis time; *1* — SiC/*p*-Si samples; *2* — SiC/*n*-Si samples.

conductance for 3 min in the enlarged scale is given in a separate Figure 8, *c*.

For easy determination of the wavelengths and peaks energies in PL spectra we have summarized the data in the table.

Locations of base PL peaks according to data in Figure 8

Sample	1 peak		2 peak	
	λ, nm	E, eV	λ, nm	E, eV
SiC/*n*-Si 1 min	395.65	3.13	496.98	2.49
SiC/*p*-Si 1 min	395.76	3.13	492.83	2.52
SiC/*n*-Si 3 min	396.91	3.12	479.54	2.59
SiC/*p*-Si 3 min	398.15	3.11	469.04	2.64
SiC/*n*-Si 5 min	396.11	3.13	496.98	2.50
SiC/*p*-Si 5 min	396.53	3.13	503.71	2.46
SiC/*n*-Si 40 min	394.87	3.14	470.85	2.63
SiC/*p*-Si 40 min	400.62	3.10	457.59	2.71

4. Discussion

From the provided experimental data and dependencies we may definitively say that the process of silicon transformation into silicon carbide in terms of substitution reaction (1) is a process of certain regularity. This regularity implies that at the moment between 1–3 min of synthesis there occurs a sharp step-like change in SiC surface layer structure, phase interface SiC-Si structure, pores density beneath SiC layer, roughness of SiC surface and also changes of some other properties. They are clearly seen in SEM images of SiC/Si(111) cross-sectional fractures and their reflection from SiC/Si(111) surface can be distinctly registered by electron diffraction analysis, photoluminescence and ellipsometry. The rigid crust and shrinkage pores are formed during the fist stage of synthesis (1 min of synthesis). These are the large pores located just behind the crust in silicon (see Figures 2 and 6). Fine pores are practically absent in this layer, the density of fine pores is minimal. According to electron diffraction analysis (RHEED images in Figure 2) the third order diffraction streaks (strands), shown by arrows, and point reflections peculiar to the transmission diffraction are visible in the electron diffraction patterns. As known from [18,19], the presence of diffraction streaks indicate possible reconstruction of the crystal surface. In study [9] it was found that depending on the method of SiC growth on Si surface the SiC surface may have the following basic structures occurring during the surface reconstruction. These are structures (1×1), (2×1), (2×2), (3×3) and structure $(\sqrt{3} \times \sqrt{3})R30^0$. On 3C-SiC(100) surface as discussed in paper [20], other types of surface reconstruction are observed, however, we do not consider this type of surface in this study. It should be emphasized that methods used in [9] for growing of SiC are the standard growth methods, i. e. these are such methods where the atoms containing Si and C are entering the Si surface from external sources. The authors of paper [9] have discovered that depending on the growth method, one of which is a solid-source molecular beam epitaxy (SSMBE), and another — method of carbonization based on the interaction of propane and hydrogen mixture with Si in the reactor of rapid thermal chemical vapor deposition (RTCVD) the RHEED images obtained from SiC/Si(111) films surface differ fundamentally. In particular, it was demonstrated that when high-energy electrons are reflected from the surface of SiC/Si(111) films two basic types of electron diffraction patterns are obtained. If SSMBE method is used for the films growth the RHEED images are similar to the images shown in the inserts in Figures 2, 4 and 5, i. e. we may observe the third order diffraction streaks (strands) on the electron diffraction patterns. If RTCVD method is used for SiC/Si(111) films growth there are no any third order diffraction streaks, and RHEED images described in [9], are equivalent to RHEED images illustrated in the inserts in Fig-

ure 3. The authors of paper [9] relying on findings from [18], demonstrated that the first type of RHEED images indicates a (3×3) Si reconstruction of SiC surface, which means that Si atoms are coming onto the surface. The type of RHEED image shown in the inserts in Figure 3 corresponds to (2×1) type of reconstruction [18], which is more common for SiC crystals with their C-faces looking upward, however, this reconstruction may also appear in Si-faces, as well. It should be noted that in order to clearly define the type of reconstruction we need to have RHEED images of SiC/Si samples not only in $\langle 110 \rangle$ azimuth, but in $\langle 112 \rangle$ azimuth, as well. There were these images that we used for defining the type of SiC/Si surface reconstruction. We can't show the images in $\langle 112 \rangle$ azimuth because of shortage of space in the page. We should only note that the image in $\langle 110 \rangle$ azimuth coincides with the image from paper [9], while images in $\langle 112 \rangle$ azimuth differ. Our image corresponds to (2×1) type of reconstruction, since there's no second order diffraction streak while in the image from the study [9] we may well see this second order diffraction streak which indicates (2×2) type of reconstruction. It should be also stressed that, according to the density functional analysis, (2×1) reconstruction for C-face is very beneficial in terms of energy. In study [21] they have experimentally found that if Si surface of (111) orientation is treated with carbon from a solid source carbon, the Si carbonization occurs in the molecular-beam epitaxy (MBE) system. As a result of this process at a temperature above 550°C, on Si(111) surface with (7×7) reconstruction the sub-monolayer SiC clusters with $(\sqrt{3} \times \sqrt{3})R30^0$ reconstruction started to arise. After that, at a temperature above 640°C during the carbonization process the $(\sqrt{3} \times \sqrt{3})R30^0$ surface reconstruction started to transform into (1×1) surface reconstruction with C atoms coming out on the surface. At that, the authors of paper [21] have found that it was this moment of time when SiC islands started to form. RHEED images obtained in this study during the process of SiC formation with (1×1) type of reconstruction and C atoms coming out to surface, correspond to RHEED images shown in Figure 3.

In paper [22] based on a strong similarity between Si(111) (7×7) and SiC(111) (3×3) reconstructions, it was suggested that in 3C-SiC(111) the reconstruction (3×3) is beneficial in terms of energy, given that during Si enrichment, both, Si-dimer configurations, and Si-adatoms configurations may take place. Finally, according to paper [23], based on the studies of SiC/Si(111) samples electron structure obtained through coordinated substitution of atoms *in situ* in the super-high vacuum by method of synchrotron photo-emission spectroscopy with photon energies within 60–400 eV, it was clearly identified that SiC/Si(111) surface is enriched with a silicon that has double Si layers, Si-dimers and Si-adatoms.

Thus, from the mentioned above analysis it follows that at the earliest atoms substitution phase (Figure 2) in our case, the surface of SiC/Si(111) samples is featuring a (3×3) reconstruction with silicon atoms showing up on the surface. This reconstruction leads to a higher size of

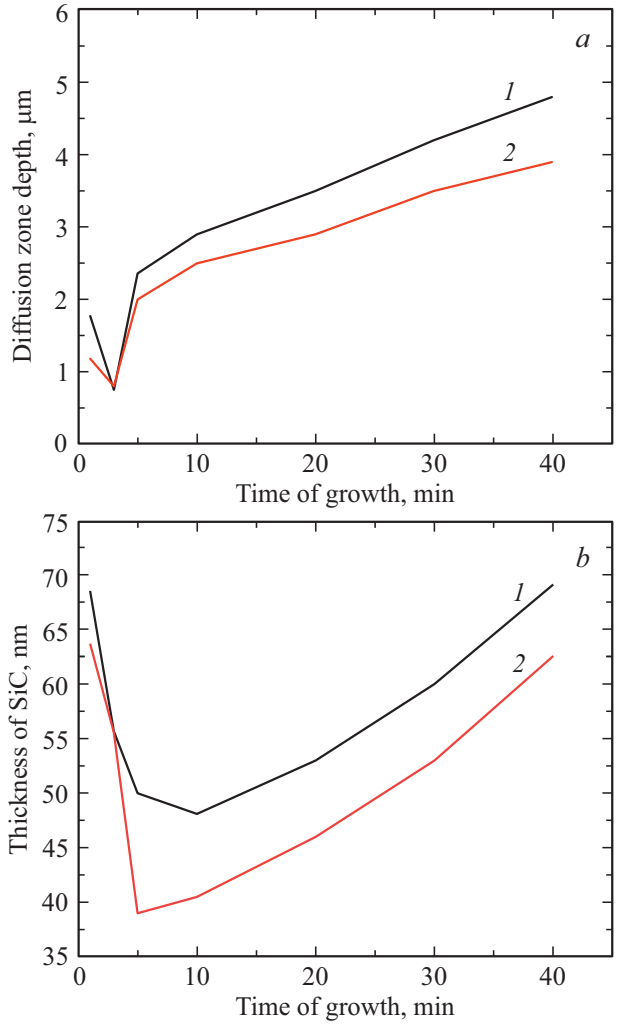

Figure 7. *a* —SiC films diffusion zone depth in SiC/Si(111) samples versus synthesis time; *1* — SiC/*p*-Si samples; *2* — SiC/*n*-Si samples. *b* — average thicknesses of SiC films in SiC/Si(111) samples versus synthesis time; *1* — SiC/*p*-Si samples; *2* — SiC/*n*-Si samples.

„cells" on the surface of SiC layer and, as a consequence, results in accelerated delivery of CO gas to the reaction volume (1) and facilitates the removal of SiO by-product from the reaction volume. After that, in the 3rd minute of synthesis a drastic change in the surface structure occurs. At this stage the surface of SiC/Si(111) samples transforms into a (2×1) reconstructed SiC surface with carbon atoms showing up on the surface. Meanwhile, as discussed above, the layer is shrinking, the size of „cells" on SiC layer surface is decreased, and access of CO to the reaction volume is decelerated.

In the fifth minute of synthesis the surface properties start changing again and the third order diffraction streaks are appearing again on the electron diffraction patterns, which indicates the formation of (3×3) structure on SiC surface with silicon atoms coming into the surface. It shall be noted that on SiC surface grown on Si of *p*-type of conductance

this process occurs faster. At that, in the inserts in Figure 3, namely insert in Figure 3, *b* we may see the point reflections specific for Si nano-islands formation.

Thus, the experiment demonstrated that between the 1st and 3d minutes of synthesis the first and basic stage of phase transformation of Si into SiC occurs, and by 5-th minute this transformation of Si into SiC is completely finished. By this time, in Si layer 70 nm thick the following has occurred: absorption of CO gas, formation of „pre-carbide" silicon, its collapse into SiC, formation of SiC layer and shrinkage pores underneath (Figure 3). At this stage the reaction (1) is decelerated, since the access of CO to the deeper Si layers is closed because of SiC layer, while SiO gas remaining in the shrinkage pores and dissolved in Si staying entrapped results in the reaction equilibrium displacement (1) to the left. However, reaction (1) still proceeds. The reaction is only slowed, because since [1–5] the nucleus of SiC at this growth stage is surrounded by vacancy clusters, through which CO is „infiltrated" into Si, while SiO goes out. CO first of all comes into the voids in silicon that have been formed during shrinkage and fills these voids. Silicon coming from silane smoothens the surface of SiC and inhibits formation of silicon vacancies V_{Si} in SiC. In pure CO the process of Si transformation in SiC occurs in similar way, however, the transformation stages periods only in the presence of pure CO differ from stages of transformation periods either in CO and silane mixture [14].

As can be seen from the micro-photoes in Figures 2–5, the pores are formed unevenly across the substrate thickness. In the start of SiC film growth the large pores are formed, both, directly near SiC-Si phase interface and slightly below the boundary of SiC-Si (Figure 2). Fine pores are practically absent. After that, at the third minute of growth (Figure 3) the density of large pores is decreased, and their sizes also go down. Along with that, fine pores start to appear. These pores are located close to SiC/Si interface and start to form also slightly below it, deep in the substrate. At the fifth minute of synthesis the density of pores sharply goes up. They start to fill the entire area of the end face cleaved surface and grow in size. While diffusion zone boundary of the chemical reaction moves deeper into the substrate. In 40th minute the density of pores is still rising. Some of them merge with each other generating large voids. As the synthesis continues the reaction decays. Further, the system remains practically unchanged. From the experimental data it follows that the process of Si transformation in SiC on substrates of *p*-type of Si and substrates of *n*-type of Si, though, running in the same way, yet, have some differences in the formation kinetics and growth. In the very first minutes of synthesis the density and sizes of pores in Si *p*-type substrate and Si *n*-type substrate are approximately equal. In the moment of shrinkage, i. e. in the third minute of synthesis some differences occur between them. The density of pores in Si *n*-type substrate drastically rises and becomes higher than the density of pores in Si *p*-type substrate (Figure 6). The area covered with shrinkage pores in Si *n*-type substrate grows lower than the area covered with shrinkage pores in *p*-type Si substrate (Figure 6). In the fifth minute of synthesis the changes occur again. The density of pores in Si *p*-type substrate starts to grow with higher rate than the density of pores in *n*-type Si substrate. By 15 min. of synthesis the densities of pores in Si *p*-type and *n*-type substrates become equal. Further, the density of pores and area occupied by pores in Si *p*-type substrate rise higher than in *n*-type substrate. In the end of the process after a 40-minute synthesis the pores density doesn't grow any longer. The pores are only enlarged in size. At that, the density of pores in *p*-type substrate is higher than the density of pores in *n*-type substrate. Figure 7, *a* illustrates the dependencies of diffusion zone movement, i. e. movement of diffusion zone deep into the Si substrate, and Figure 7, *b* illustrates the SiC films thicknesses versus time. These dependencies also correlate with the dependencies described above shown in Figure 6, i. e. the rate of diffusion flank movement into Si *p*-type substrate after five minutes of synthesis occurs faster than in Si *n*-type substrate. Up to this time their rates are equal. The thicknesses of SiC films (Figure 7, *b*) at the start of synthesis are comparable, then, in the 3d minute of synthesis a more intensive shrinkage of SiC layer on Si substrate of *n*-type occurs. Only in the 40th minute of synthesis the films thicknesses on both types of substrates become comparable.

So, formation of pores in Si substrate, i. e. increase of their density and sizes occurs more intensively inside the Si substrate of *p*-type, under the layer of SiC. At the same time the density of vacancies V_{Si} in SiC layer grown on *n*-type Si substrate is higher than in SiC synthesized on Si substrate of *p*-type of conductance and energy of their embedding in the band gap is higher. This fact proves the earlier made theoretical findings [25,26] and experimentally identified [15] difference in reaction (1) on Si substrates of p and *n*-types of conductance. Thus, in the study [15] it was found that in SiC films grown on Si(111) of *n*-type of conductance, and in SiC films grown on Si(111) of *p*-type of conductance for 1 min the elastic compressing deformations arise. After that, at stage 3–5 min of the synthesis these deformations start growing. Whereas in SiC films synthesized on Si(111) of *p*-type of conductance the compressing deformations are replaced by tensile deformations. After that in SiC films synthesized on Si(111) of *n*-type of conductance the compressing deformations are fully relaxed. The elastic deformations in SiC films grown on Si(111) of *p*-type of conductance are fully relaxed only to the 40th minute of synthesis.

The cause of these differences was studied in details in paper [25] and is explained by the fact that mechanism of reaction (1) greatly depends on the presence of *n*-type or *p*-type impurities in the original silicon substrate which define the charge of silicon vacancy in SiC. If Si substrate is heavily doped with *n*-type impurity, (phosphorous atoms here) then, it may happen that in Si heavily doped with *n*-type impurity the carbon won't go entirely to the silicon vacancy V_{Si} [25]. This means that the stage of pre-carbide silicon collapse will

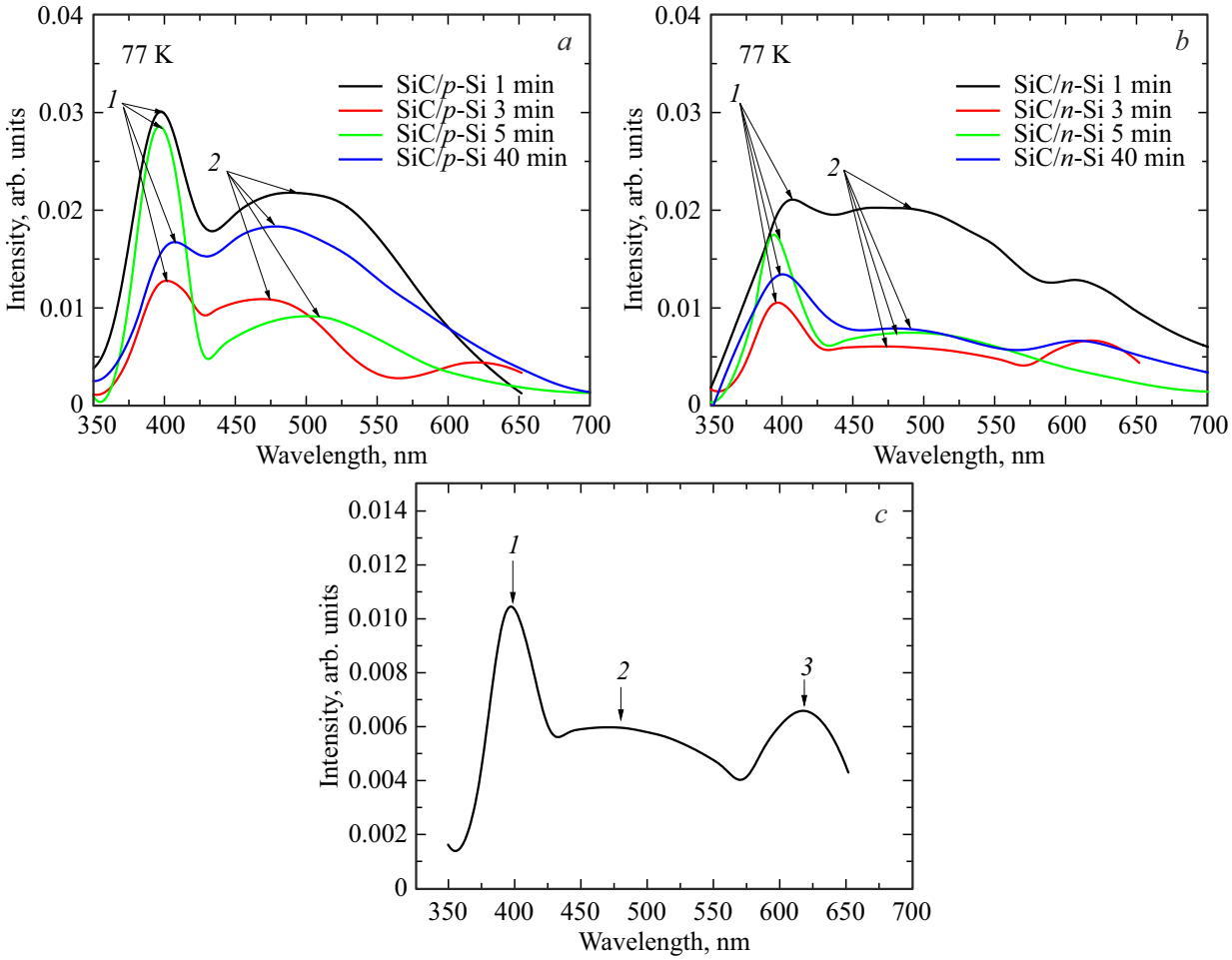

Figure 8. Photoluminescence spectra from SiC/Si(111) samples obtained in different time of SiC synthesis on Si(111) substrates of *n*- and *p*-type of conductance; *a* — SiC on Si of *p*-type of conductance; *b* — SiC on Si of *n*-type of conductance; *c* — photoluminescence spectrum with peaks equal to: 396.91 (*1*), 479.54 (*2*) and 630.26 nm (*3*) of SiC sample synthesized on Si substrate of *n*-type of conductance for 3 min.

go more slowly. As a result, in SiC layer grown on Si of *n*-type of conductance, the silicon vacancies are formed, but not in silicon as it was in the beginning of reaction (1), but in silicon carbide V_{Si}. Thus, the type of doping impurity leads to asymmetry of intermediate stages of reaction (1), which of course will impact the structure of the formed SiC layers. This conclusion is clearly confirmed by PL spectra given in Figure 8.

From Figure 8, *a* and *b* it follows that PL spectra of SiC layers vary significantly. The most noticeable changes occur during initial stages of synthesis. Noticeable changes also occur in behavior of PL spectra of SiC layers grown on Si substrates of *n*-type and *p*-type of conductance. It is difficult to interpret the SiC layers luminescence spectra first of all because silicon carbide is not a direct-band-gap semiconductor. Moreover, the hybrid structure contains not only SiC/Si heterojunction, but also can be comprised of thin layers of different SiC polytypes [1–5], which, in their turn, may form a system of heterojunctions. From the analysis of samples diffraction patterns described in paper [15], and their PL spectra shown in Figure 8, we may see that a cubic polytype is prevailing 3C-SiC.

According to Figure 8, the PL spectra of SiC/Si structures, in general, apart from SiC sample spectra, grown on Si of *n*-type of conductance for 1 min, consist of peaks with maximums 395.76 nm ($h\nu = 3.13$ eV), wide band with maximum from 471 nm ($h\nu = 2.63$ eV) to 520 nm ($h\nu = 2.38$ eV) with bend („shoulder“) within the wavelengths of 430 nm ($h\nu = 2.88$ eV). The exact wavelengths and energies of these domains are given in Table. Among the PL spectra the most distinguished one is the spectrum of SiC sample, grown on Si of *n*-type of conductance for 1 min. It has a blurred peak in 410 nm ($h\nu = 3.02$ eV) domain, a small „shoulder“ in 450 nm ($h\nu = 2.76$ eV) domain, blurred wide band with maximum in 500 nm ($h\nu = 2.48$ eV) and a small peak in 623 nm ($h\nu = 1.99$ eV). The PL spectrum of SiC layer grown on Si of *p*-type of conductance for 1 min is similar to spectrum of SiC layer grown on Si substrate of *n*-type of conductance, but its peaks have a more pronounced shape. The type of this spectrum indicates a more distinct

structure of SiC on Si of *p*-type of conductance, compared to SiC on Si of *n*-type of conductance. Here, the first peak (395.76 nm), „shoulder" (425 nm) and band with maximum in 492.83 nm domain can be clearly seen. Thus, the PL spectra also prove the presence of differences in kinetics of SiC layers formation on Si substrates of *p*- and *n*-types of conductance.

In the process of synthesis of SiC layers, similar to all other parameters of SiC structure, the PL spectra also undergo sufficient changes. The most noticeable changes can be observed for SiC sample on Si substrate of *p*-type of conductance, that has been synthesized for 5 min. The first peak shifts slightly to the right (396.11 nm),becomes more narrow and pronounced. The intensity of wide band goes down and it becomes more shallower. For SiC sample on Si of *n*-type of conductance this streak is almost completely smoothed out. With further synthesis (40 min) the shape of PL spectrum partially returns to the shape of spectrum for a sample synthesized during 1 min, i. e. the nature of PL spectra variation entirely complies with the type of changes of all basic characteristics shown in Figures 2–8. It should be noted that in the third minute of synthesis in PL spectra of samples a peak in 623.05 nm range has appeared for SiC sample on Si of *p*-type of conductance and in 630.26 nm range for SiC/*n*-Si. This peak is especially noticeable on SiC/*p*-Si sample, therefore, the PL spectrum for this sample is shown in the separate Figure 8, *c*. It should be noted that the peak corresponding to PL spectrum in this domain is shifted towards the shorter wavelength for SiC/*n*-Si samples compared to SiC/*p*-Si samples. With regards to SiC/*p*-Si sample that was grown during the third minute of synthesis, the peak in 395.76 nm domain can be attributed as excitonic in a mixture of cubic and hexagonal phases, since this peak is quite narrow and located on a short-wave edge of the wide streak [27]. The bend („shoulder") in the area of about 425–430 nm, probably, belongs to 6H polytype. Slit band with even more intense and wide streak of maximum about 500 nm, the details of which cannot be viewed. The streak of about 425–430 nm is clearly not an excitonic one — it is quite wide, therefore it shall be called an „edge luminescent" streak, i. e. a mix of transitions of various kinds, however, more or less corresponding to the zone edge in terms of the energy.

The streaks in 623 nm ($h\nu = 1.99$ eV) domain can be interpreted as a 3C-SiC polytype, similar to [28] or as a silicon vacancy with deep level of embedment in 630 nm ($h\nu = 1.97$ eV) band gap for SiC/*n*-Si sample. For a more precise analysis of PL spectra it is required to etch the Si substrate, as it was made in study [28], which is suggested to be fulfilled later.

5. Conclusion

This study included a comprehensive research of the processes of evolution of structure and surface properties of single-crystal Si with its coordinated transformation into epitaxial Si layer. It was experimentally identified that during Si conversion into SiC a chemical synthesis of the new phase molecules inside the old phase takes place with its further collective first-order phase transition into a crystalline phase of a new type. It was found that the process of SiC new phase formation can be conventionally divided in two stages. During the first synthesis stage (about 1 min of synthesis) a layer of SiC is formed, saturated with residual partially reacted silicon vacancies and large shrinkage pores formed in SiC/Si interface. Fine pores are practically absent during this stage. At that, the reconstructed surface of SiC/Si(111) samples is featuring (3×3) structure with the silicon atoms showing up on the surface.

During the second synthesis stage at the moment between 1–3 min there occurs a significant change in SiC surface layer structure, change in the phase interface SiC-Si structure, pores density beneath SiC layer, roughness of SiC surface and also changes of some other properties. SiC layer becomes compact, and the number of vacancies is minimal. At this stage the density of large pores is decreased, and the size of pores is reduced as well. Along with that, fine pores start to appear near SiC-Si interface. The surface structure also undergoes noticeable changes. At this stage the reconstructed SiC surface with a (3×3) structure and silicon atoms showing up is being transformed into SiC surface with (2×1) structure and carbon atoms appearing on the surface. At this stage, along with the layer structure, all other basic physical properties of hybrid SiC/Si substrates also change, namely, their optical properties. SiC layer here is elastically compressed by the substrate.

At this stage the reaction (1) is decelerated, since the access of CO to the deeper Si layers is closed because of SiC layer, while SiO gas remaining in the shrinkage pores and dissolved in Si staying entrapped results in the reaction equilibrium displacement (1) to the left. However, here, during shrinkage and structure layer transformation the CO gas is starting to be „entrapped" deep into Si. CO comes into the voids in silicon that have been formed during shrinkage and fills these voids. It is this moment, when the third and final stage in formation of SiC on Si occurs. At this stage the SiC/Si diffusion zone in silicon is generated under SiC layer. The pores start intensively form and grow under SiC layer. In the 5th min of synthesis the density of fine pores increases in a step-like manner. At this moment the elastic compressive deformations become zero, because of the vacancy „swelling" of the material. (2×1) structure is replaced by (3×3) structure. Carbon atoms on SiC surface are substituted by Si atoms. A smooth growth of the pores begins, and diffusion flank of the chemical reaction moves deeper into the substrate. At this stage, in SiC layer the elastic tensile deformations arise, which, to the 40 min become fully relaxed. It is evident, that tensile deformations arise because of material „swelling" under SiC layer resulting in tension of SiC layer. Here cracks, fine pores and vacancies may be formed through which CO gas will gradually seep into and SiO gas as a reaction product will go out.

It was found that in Si substrates of *p*- and *n*-types of conductance the processes of SiC formation occur similarly. There are only small differences in kinetics of Si transformation into SiC.

Funding

This study was supported by grant No. 23-91-01001 from the Russian Science Foundation. The research was carried out using the equipment of the unique scientific facility „Physics, Chemistry and Mechanics of Crystals and Thin Films“ of Institute for Problems in Mechanical Engineering of the Russian Academy of Sciences, Federal State Unitary Enterprise (St. Petersburg).

Conflict of interest

The authors declare that they have no conflict of interest.

References

[1] S.A. Kukushkin, A.V. Osipov. J. Phys. D **47**, 313001 (2014). DOI: 10.1088/0022-3727/47/31/313001
[2] S.A. Kukushkin, A.V. Osipov, N.A. Feoktistov. FTT **56**, *8*, 1457 (2014). (in Russian). DOI: 10.1134/S1063783414080137
[3] S.A. Kukushkin, A. V. Osipov. Inorganic Materials **57**, *13*, 1319 (2021). DOI: 10.1134/S0020168521130021
[4] S.A. Kukushkin, A.V. Osipov. Russ. J. Gen. Chem. **92**, *4*, 547 (2022). DOI: 10.1134/S1070363222040028.
[5] S.A. Kukushkin, A.V. Osipov. Kondensirovannye sredy i mezhfaznye granitsy, **24**, *4*, 407 (2022). (in Russian). DOI: 10.17308/kcmf.2022.24/10549
[6] A. Severino, C. Locke, R. Anzalone, M. Camarda, N. Piluso, A. La Magna, S. Saddow, G. Abbondanza, G. D'Arrigo, F. La Via. ECS Trans. **35**, *6*, 99 (2011). DOI: 10.1149/1.3570851
[7] G. Ferro. Crit. Rev. Solid State Mater. Sci. **40**, *1*, 56 (2015). DOI: 10.1080/10408436.2014.940440
[8] S. Nishino, J.A. Powell, H.A. Will. Appl. Phys. Lett. **42**, *5*, 460 (1983). DOI: 10.1063/1.93970
[9] J. Pezoldt, Th. Kups, Th. Stauden, B. Schröter. Mater. Sci. Eng. B **165**, 28 (2009). DOI: 10.1016/j.mseb.2009.03.015
[10] F. Iacopi, G. Walker, L. Wang, L. Malesys, Sh. Ma, B.V. Cunning, A. Iacopi. Appl. Phys. Lett. **102**, 011908 (2013). DOI: 10.1063/1.4774087
[11] S.A. Kukushkin, A.V. Osipov. Zhurn. neorgan. khimii (2024). (in Russian). V pechati.
[12] S.A. Kukushkin, A. V. Osipov, E.V. Osipova. Tech. Phys. Lett. **48**, *10*, 78 (2022). DOI: 10.21883/TPL.2022.10.54806.19310).
[13] S.A. Kukushkin, L.K. Markov, A.S. Pavlyuchenko, I.P. Smirnova, A.V. Osipov, A.S. Grashchenko, A.E. Nikolaev, A.V. Sakharov, A.F. Tsatsulnikov, G.V. Sviatets. Coatings **8**, *7*, 1142 (2023). DOI: 10.3390/coatings13071142
[14] S.A. Kukushkin, A.V. Osipov, E.V. Osipova, V.M. Stozharov. Phys. Solid State **64**, *3*, 327 (2022). DOI: 10.21883/PSS.2022.03.53187.232
[15] I.A. Eremeev, M.G. Vorobev, A.S. Grashchenko, A.V. Semencha, A.V. Osipov, S.A. Kukushkin. Phys. Solid State **65**, *1*, 68 (2023). DOI: 10.21883/PSS.2023.01.54976.480
[16] L.K. Markov, S.A. Kukushkin, I.P. Smirnova, A.S. Pavlyuchenko, A.S. Grashchenko, A.V. Osipov, G.V. Svyatets, A.E. Nikolayev, A.V. Sakharov, V.V. Lundin, A.F. Tsatsulnikov. Pis'ma v ZhTF **47**, *18*, 3 (2021). (in Russian). DOI: 10.21883/PJTF.2021.18.51462.18877
[17] I.P. Kalinkin, S.A. Kukushkin, A.V. Osipov. Semiconductors **52**, 802 (2018). DOI: 10.1134/S1063782618060118.
[18] A. Fissel. Phys. Rep. **379**, 147 (2003). DOI: 10.1016/S0370-1573(02)00632-4
[19] V.V. Balashev, V.V. Korobtsov, T.A. Pisarenko, L.A. Chebotkevich, N.N. Galkin FTT **52**, *2*, 370 (2010). (in Russian).
[20] A.Yu. Aristov. UFN **171**, *8*, 801 (2001). (in Russian). DOI: 10.3367/UFNr.0171.200108a.0801
[21] V. Cimalla, Th. Stauden, G. Ecke, F. Scharmann, G. Eichhorn, J. Pezoldt, S. Sloboshanin, J. A. Schaefer. Appl. Phys. Lett. **73**, 3542 (1998). DOI: 10.1063/1.122801
[22] J. Schardt, J. Bernhardt, U. Starke, K. Heinz. Phys. Rev. B **62**, 10335 (2000). DOI: 10.1103/PhysRevB.62.10335.
[23] G.V. Benemanskaya, P.A. Dementev, S.A. Kukushkin, M.N. Lapushkin, A.V. Osipov, B. Senkovskiy, S.N. Timoshnev. Mater. Phys. Mech. **22**, 183 (2015).
[24] R. Kaplan. Surf. Sci. **215**, *1–2*, 111 (1989). DOI: 10.1016/0039-6028(89)90704-8
[25] S.A. Kukushkin, A. V. Osipov. Materials **15**, 4653 (2022). DOI: 10.3390/ma15134653
[26] S.A. Kukushkin, A.V. Osipov, I.P. Soshnikov. Rev. Adv. Mater. Sci. **52**, 29 (2017).
[27] M.E. Kompan, I.G. Aksyanov, I.V. Kulkova, S.A. Kukushkin, A.V. Osipov, N.A. Feoktistov. FTT **51**, *12*, 2326 (2009) (in Russian).
[28] H.W. Shim, K.C. Kim, Y.H. Seo, K.S. Nahm, E.-K. Suh, H.J. Lee, Y.G. Hwang. Appl. Phys. Lett. **70**, *13*, 31 1757 (1997). DOI: 10.1063/1.118648

Translated by T.Zorina